

## 2. DIFFRACTION GEOMETRY AND ITS PRACTICAL REALIZATION

## 2.3.3.1.2. Crystallite-size effects

In addition to profile broadening, which begins to appear when the crystallite sizes are  $< 1\text{--}2\ \mu\text{m}$ , the sizes have a strong effect on the absolute and relative intensities (de Wolff, Taylor & Parrish, 1959; Parrish & Huang, 1983). The particle sizes have to be less than about  $5\ \mu\text{m}$  to achieve 1% reproducible relative intensities from a stationary specimen in conventional diffractometer geometry (Klug & Alexander, 1974). The statistical errors arising from the number of particles irradiated can be greatly reduced by using smaller particles and rotating the specimen around the diffraction vector. This brings many more particles into reflecting orientations.

The particle-size effect is illustrated in Fig. 2.3.3.2 for specimens of NIST silicon standard powder 640 sifted to different size fractions. The powders were packed in a 1 mm deep cavity in a 25.4 mm diameter Al holder using 5% collodion/amyl acetate binder. They were rotated by a synchronous motor (a stepper motor can also be used) around the axis normal to the centre of the specimen surface with the detector arm fixed at the peak position and the intensity recorded with a strip-chart. Rapid rotation,  $\sim 60\ \text{r min}^{-1}$ , gives the average peak intensity for all azimuths of the specimen and the small variations result only from the counting statistics. Scaling the intensities to  $(111) = 100\%$  for the  $5\text{--}10\ \mu\text{m}$  fraction, the  $10\text{--}20\ \mu\text{m}$  fraction is 94%,  $20\text{--}30\ \mu\text{m}$  88% and  $> 30\ \mu\text{m}$  59%. The decrease is probably due to lower particle-packing density and increasing interparticle microabsorption. The  $> 5\ \mu\text{m}$  fraction = 95% may be due to the larger ratio of oxide coating around the particles to the mass of the particles.

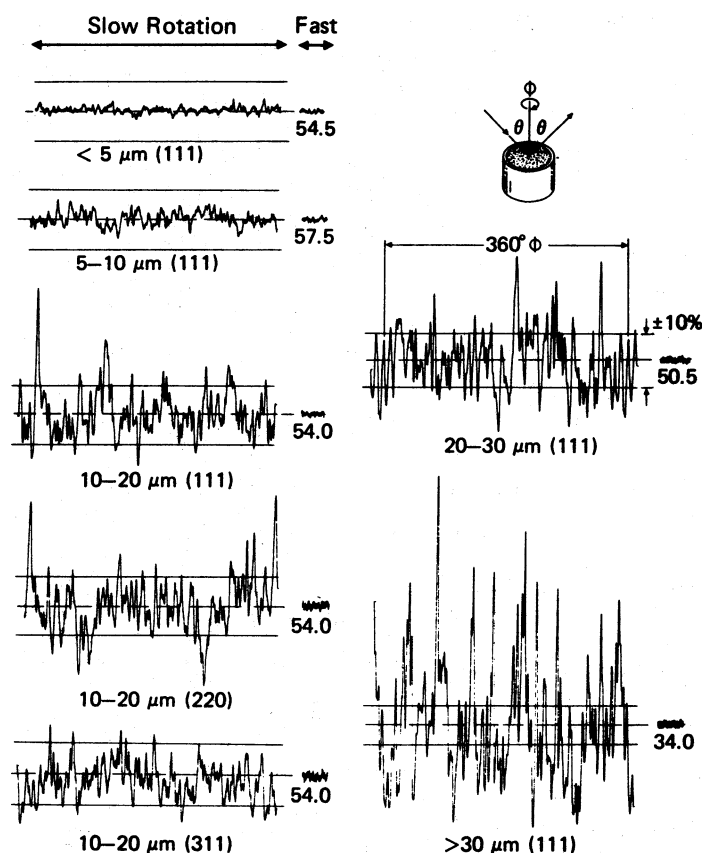


Fig. 2.3.3.2. Effect of specimen rotation and particle size on Si powder intensity using a conventional diffractometer (Fig. 2.3.1.3) and Cu  $K\alpha$ . Numbers below fast rotation are the average intensities.

Slow rotation,  $\sim 1/7\ \text{r min}^{-1}$ , shows the variation of the peak intensity with azimuth angle  $\varphi$ . The pattern repeats after  $360^\circ$  rotation and the magnitude of the fluctuations increases with increasing particle sizes and resolution. There is no correlation between the fluctuations of different reflections, as can be seen by comparing the 111, 220 and 311 reflections of the  $10\text{--}20\ \mu\text{m}$  specimen (lower left side) for which the incident-beam intensity was adjusted to give the same average amplitude. The horizontal lines are  $\pm 10\%$  of the average. This shows the magnitude of errors that could occur using stationary specimens. Similar particle-size effects were found using the integrated intensities derived from profile fitting. The above discussion and Fig. 2.3.3.2 refer to a continuous scan. If the step-scan mode is used to collect data, it is clearly not necessary to rotate the specimen through more than one revolution at each step.

The rotating specimen also averages the in-plane preferred orientation but has virtually no effect on the planes oriented parallel to the specimen surface. The slow rotation method is useful in testing the grinding and sifting stages in specimen preparation. When calibrated with known size fractions, it can be used as a rough qualitative measure of the particle sizes.

2.3.3.2. Problems arising from the  $K\alpha$  doublet

A common source of error arises from the  $K\alpha$  doublet which produces a pair of peaks for each reflection. The separation of the Cu  $K\alpha_1$ ,  $K\alpha_2$  peaks increases from  $0.05^\circ$  at  $20^\circ 2\theta$  to  $1.08^\circ$  at  $150^\circ 2\theta$ . The overlapping is also dependent on the instrument resolution and may cause errors in the peak angles and intensities when strip-chart recording or peak-search methods (described below) are used. The  $K\alpha_1$  wavelength is generally used to calculate all the  $d$ 's even when the low-angle peaks are unresolved. In the region where the doublet is only slightly resolved, the apparent  $K\alpha_1$  peak angle is shifted to higher angles because of the overlapping  $K\alpha_2$  tail and similarly the peak intensities will be in error. The relative peak intensities of a reflection with superposed doublet compared to a resolved doublet could have an error as large as 50%. Relative peak intensities are used in the ICDD standards file and cause no problem because the unknowns are measured in the same way. The integrated intensity avoids this difficulty but is impractical to use in routine identification.

Rachinger (1948) described a simple graphical procedure for removing  $K\alpha_2$  peaks. The method causes errors because it makes the incorrect assumption that  $K\alpha_2$  is the exact half-scale version of  $K\alpha_1$ . Ladell, Zagofsky & Pearlman (1975) developed an exact algorithm using the actual mathematical shapes observed with

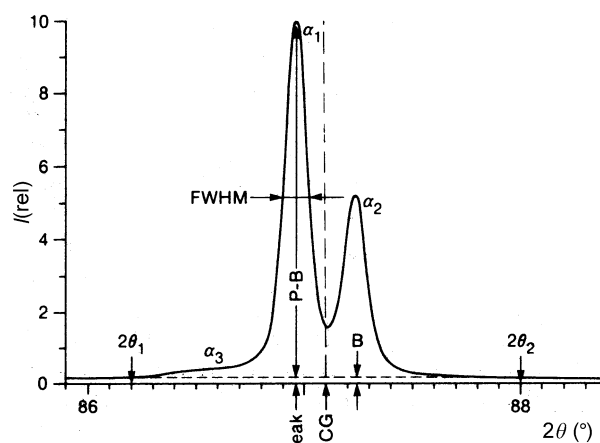


Fig. 2.3.3.3. Various measures of profile.